

Intercalant vibrations in a graphite intercalation compound observed by infrared reflectivity at a graphite-germanium interface

Franz Jost, Yizhak Yacoby,* Detlev Heitmann, and Siegmund Roth

Max-Planck-Institut für Festkörperforschung, Heisenbergstrasse 1, D-7000 Stuttgart 80, Bismarckstrasse 80, Federal Republic of Germany

(Received 1 September 1988)

We report on a new method to observe intercalant vibrations in graphite intercalation compounds (GIC) using ir reflectivity. It is shown that, under certain conditions, phonons affect the reflectivity, at an interface between an ir-transparent material (IRTM) and an intercalated graphite sample, much more than at an air-sample interface. The results of reflectivity measurements as a function of the angle of incidence support the theoretical analysis and provide the dielectric tensors for pure highly oriented pyrolytic graphite and for stage-1 C/AsF₅ GIC samples. Using these results we calculate the relative sensitivity of reflectivity spectra to phonon contributions as a function of the angle of incidence. We show that the sensitivity has a maximum at an angle θ_c for which the electromagnetic radiation in the graphite propagates parallel to the graphite surface. We also present *in situ* measurements of the reflectivity as a function of photon energy. The spectra display the evolution of the A_{2u} mode at different intercalation times as well as five lines which correspond to vibrations of AsF₃, AsF₅, AsF₆⁻, and possibly As₂F₁₁⁻. The line shapes are also clearly explained.

I. INTRODUCTION

The observation of intercalant vibrational frequencies has been difficult both in Raman and in ir reflectivity measurements. While in Raman reflectivity a general method has been found which facilitates the observation of intercalant vibrational modes,¹ the use of ir reflectivity still presents difficulties. In graphite and, in particular, in graphite intercalation compounds (GIC's) the reflectivity is essentially governed by the free carriers strongly dominating the small contribution of the phonons. Consequently the small phonon contributions cannot be seen. In this paper we present a new method for observing intercalant vibrations in GIC's, using infrared-reflectivity measurements.

The lattice dynamics of graphite have been thoroughly investigated both theoretically and experimentally.² Graphite has four atoms per unit cell. Thus it has altogether 12 phonon branches. At the center of the Brillouin zone it has six different vibrational frequencies. Two Raman-active, two ir-active, and two silent modes. All the zone center vibrational modes had been experimentally observed. In particular, the ir-active modes of graphite have been observed by several authors³⁻⁵ and their frequencies are 868 and 1588 cm⁻¹.

Upon intercalation the dynamical properties of the intercalated compounds are expected to change in several ways.² The size of the Brillouin zone increases both in the basal plane and along the *c* axis. Thus in principle the vibrational branches fold back many times giving rise to a large number of zone center modes which should be detectable by optical methods. Dresselhaus and Dresselhaus² claim that the Raman mode at 600 cm⁻¹ in stage 1 alkali is a folded *M* point. So far the only effect of zone folding which has been observed in *all* GIC's is associated with the folding along the *c* axis.⁶ In Raman

scattering at stages $n > 2$, one observes two lines near 1600 cm⁻¹. One line corresponds to the vibration of an interior graphite layer, the other, to the vibration of a graphite layer adjacent to an intercalant layer.⁶ The difference between the E_{2g} mode frequencies of the bounding and the interior layers is about 20 cm⁻¹. Such a splitting has also been observed in the A_{2u} ir-active mode in C/HNO₃.⁷ However, the observed splitting has been only 6 cm⁻¹ in agreement with the calculations of Algishi and Dresselhaus.⁸ In addition to changes in the vibrations of the graphite layers, one expects to find the internal vibrations of the intercalant molecules as well as their vibrations relative to the graphite layers. The vibrations of alkali ions relative to the carbon lattice have been observed by neutron scattering⁹ but the other vibrations have been observed only in very few instances.

It should be stressed that observing the intercalant modes is important in several ways: It can provide information on the actual species present in the intercalant layers; it may provide information on how they are stacked and finally if the experiment is done *in situ* it may provide information on the intercalation process and on structural phase transitions. A beautiful example of such an investigation is the study of Br₂-intercalated graphite.^{10,11}

A successful method for observing intercalant vibrations was developed by Conrad and Strauss.⁷ It consists of preparing a 50- μ m-thick GIC sample, cut with its surface *perpendicular to the a axis* and measuring its ir transmission spectrum. This method gave very nice spectra. However, the sample preparation is exceedingly difficult and it can be used only for stable compounds.

In this paper we propose a new method for measuring intercalant vibrational frequencies. It consists of measuring the ir reflectivity at the interface between an ir transparent material (IRTM) such as germanium and the *c*

surface of a GIC sample. We shall show that under certain well-defined conditions such an experiment leads to a significant enhancement of the intercalant vibrations signal as compared to ordinary normal incidence reflectivity measurements.

Our paper is organized as follows: In Sec. II we analyze the reflectivity at an interface between an IRTM and a GIC. In this section we determine the conditions for highest sensitivity in observing vibrational modes. In Sec. III we describe the setup for *in situ* measurements of the reflectivity as a function of the angle of incidence. These measurements are necessary in order to determine the parameters for the spectral measurements in which the intercalant vibrations are actually studied. The experimental results are fitted theoretically and from the fit parameters we calculate the sensitivities for observing intercalant vibrational modes. The spectral measurements and the experimental results are described in Sec. IV. The observed spectra are discussed and interpreted in Sec. V. A brief summary and conclusions are provided in Sec. VI.

II. THE REFLECTIVITY AT THE INTERFACE OF AN IR TRANSPARENT MATERIAL AND GRAPHITE

Graphite-intercalation compounds are very anisotropic materials. Electrons or holes are quite free to move in the basal plane. Perpendicular to this plane, in particular, in acceptor-type compounds, the mobility is very low. The ratio between the conductivities parallel and perpendicular to the basal plane is of the order of 10^6 . This anisotropy reflects itself also in the optical dielectric function. Perpendicular to the c face ϵ_{\perp}^G is conventional, namely, its real part is positive and not very large. Parallel to the c face, ϵ_{\parallel}^G is dominated by the plasma oscillations and can be expressed in the following form:

$$\epsilon_{\parallel}^G = \epsilon_0 - \frac{\omega_p^2}{\omega^2 - i\omega\gamma}, \quad (1)$$

where ω_p is the plasma frequency, γ a phenomenological damping constant, and ϵ_0 is the high-frequency dielectric constant.

In the frequency range of the vibrational modes, which is of interest here, we are below the plasma edge. Thus the real part of the dielectric constant is negative and large. Under these circumstances and assuming a limiting case of a zero imaginary part, the reflectivity from the surface is unity for any angle of incidence.

The basic idea proposed here is to take advantage of this large anisotropy so as to obtain a large sensitivity to the phonon contributions in the reflectivity spectra.

We consider a plane EM wave with wave-vector \mathbf{K} incident at an angle θ with respect to the normal to the interface as shown in Fig. 1(a). We assume that the light is polarized with the electric-field vector in the plane of incidence. The other polarization is less interesting because the reflectivity in this case depends on ϵ_{\perp}^G only. The parallel component of the wave K_{\parallel} is of course the same for the incident, reflected and transmitted waves. Using

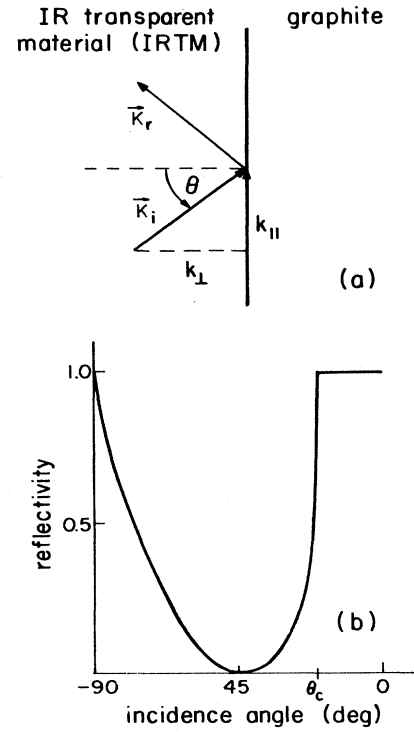


FIG. 1. (a) Reflectivity measurement diagram. \mathbf{K}_i and \mathbf{K}_r are the wave vectors of the incident and reflected beams, respectively. (b) The reflectivity as a function of the incidence angle for an extreme case of a real graphite dielectric tensor. $\epsilon_{\parallel}^G < 0$; $\epsilon_{\perp}^G > 0$.

EM wave theory we find that the wave-vector components on both sides of the interface obey the following relations. On the IRTM side,

$$K_{\perp}^2 + K_{\parallel}^2 = \omega^2 \mu \epsilon, \quad (2)$$

where ϵ is the dielectric constant of the IRTM. On the graphite side,

$$K_{\perp}^{G2} \epsilon_{\perp}^G / \epsilon_{\parallel}^G + K_{\parallel}^2 = \omega^2 \mu \epsilon_{\perp}^G, \quad (3)$$

we define an admittance Y to be the ratio between the parallel components of the magnetic and electric fields. Thus on the IRTM side,

$$Y = H/E_{\parallel} = (K_{\perp} + K_{\parallel}^2/K_{\perp})/\omega\mu. \quad (4)$$

The corresponding admittance on the graphite side is

$$Y^G = H^G/E_{\parallel}^G = (K_{\perp}^G + K_{\parallel}^2 \epsilon_{\parallel}^G / K_{\perp}^G \epsilon_{\perp}^G) / \omega\mu. \quad (5)$$

The reflection coefficient which is the ratio between the reflected and incident electric fields is then expressed in the form

$$\Gamma = (Y - Y^G)/(Y + Y^G) \quad (6)$$

and the reflectivity is given by

$$R = |\Gamma|^2. \quad (7)$$

To understand the angular dependence of the reflectivity we consider first the ideal case, namely we assume that the imaginary part of the dielectric constant is zero. Since we are interested in frequencies which are below the plasma edge, $\epsilon_{\parallel}^G < 0$. Thus if $\epsilon < \epsilon_{\perp}^G$, K_{\perp}^{G2} is negative for any K_{\parallel} consistent with Eq. (2). This is, in fact, the case when the IRTM is air. Consequently the reflectivity is equal to unity for any incidence angle θ . If on the other hand $\epsilon > \epsilon_{\perp}^G$, for $K_{\parallel}^2 > \omega^2 \mu \epsilon_{\perp}^G$, K_{\perp}^{G2} is positive. In this case the reflectivity can become less than unity, namely *the EM wave propagates in the graphite sample*.

We shall refer to the angle of incidence which satisfies the above condition as the critical angle defined as:

$$|\mathbf{K}|^2 \sin^2 \theta_c = \omega^2 \mu \epsilon_{\perp}^G. \quad (8)$$

The reflectivity as a function of the incidence angle is shown for this ideal case in Fig. 1(b). If the beam is close to normal incidence it is totally reflected. Above the critical angle θ_c , the reflectivity becomes less than unity. θ_c is a very special angle. At this angle, the EM wave in the graphite propagates parallel to the surface and its electric field is perpendicular to the surface. Namely, it is completely insensitive to the negative parallel component of the dielectric tensor. Notice that under these ideal conditions the reflectivity becomes even zero for a certain angle θ_b .

To find the sensitivity of the reflectivity to changes in the dielectric constant, we have to calculate the derivative $dR/d\epsilon^G$ for different components of ϵ^G . It is easily seen from Eqs. (4)–(6) that changes in ϵ_{\parallel}^G affect the reflectivity only very little. On the other hand, a change in ϵ_{\perp}^G has a large effect on the reflectivity with the derivative approaching infinity at the critical angle. In Sec. III we shall present a series of experiments which confirm the theoretical considerations of this section. The experiments also provide us with the actual parameters of the system. This allows us to calculate and optimize the sensitivity of the reflectivity system to vibrational features.

III. DEPENDENCE OF REFLECTIVITY ON THE ANGLE OF INCIDENCE

A. Experimental

The measurement of the reflectivity as a function of the incidence angle is performed during *in situ* doping. This *in situ* procedure was chosen because the GIC sample can be kept in a well-defined stage only if the vapor pressure of the intercalant is maintained. The intercalation unit is described in Fig. 2. The sample is attached to the germanium half-cylinder. When the graphite is thin enough (less than 50 μm) it easily attaches itself to the germanium surface. A circular chamber is pressed to the flat surface of the germanium half-cylinder. Using a viton O ring between them, the germanium and the chamber define a hermetically sealed volume in which the intercalation takes place. To perform the ir reflectivity measurement, the sample is pressed to the germanium surface using a viton cylinder. The pressure is released to continue the intercalation. The motions of the viton cylinder are controlled by the pressing screw through the pressing

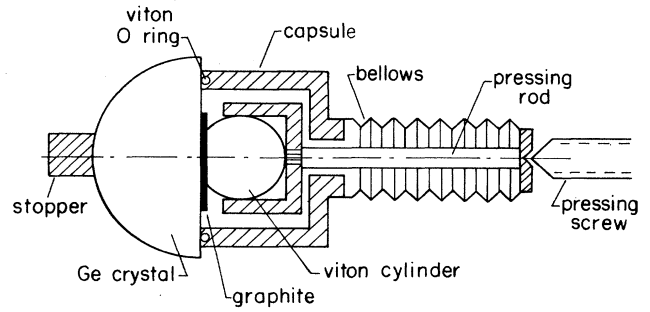


FIG. 2. The intercalation chamber for the *in situ* measurements.

rod. The bellows facilitates the motion of the pressing rod while keeping the intercalation chamber air tight.

The system for measuring the reflectivity as a function of the incidence angle is shown in Fig. 3. The ir light emanating from the monochromator is focused on the sample using a ZnSe lens. This lens is transparent to both ir and visible light. The ir light penetrates into the germanium and is reflected from the graphite germanium interface. The light is then focused by a germanium lens onto a Golay cell detector.

The system is aligned using a He-Ne laser. The laser light is focused by a cylindrical lens which is placed at a focal length distance from the center of the Ge cylinder. Thus, if the system is properly aligned the laser reflected from the cylinder's surface retraces back to the laser and to the exit slit of the monochromator independently of the angle of incidence relative to the graphite plane (see the heavy line in Fig. 3). The two slits are used in order to limit the divergence of the ir beam. This improves the accuracy of the measurement.

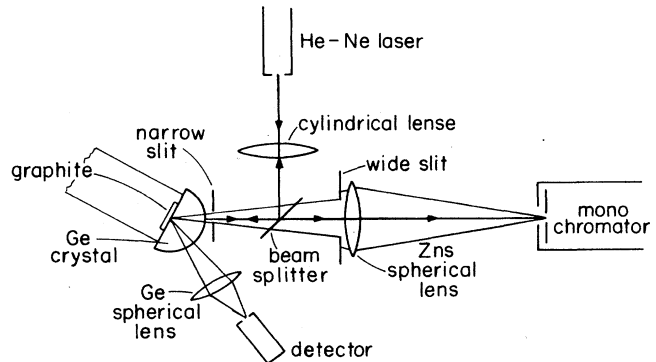


FIG. 3. Schematic diagram of the setup for the measurement of reflectivity as a function of the angle of incidence. The heavy lines with the arrows represent the path of He-Ne laser light; The light lines represent the ir beam.

B. Experimental results and analysis

The measurements were carried out on highly oriented pyrolytic graphite (HOPG) samples, intercalated with AsF_5 . The wavelength was $5 \mu\text{m}$. Other wavelengths were also used but their results are consistent with the $5\text{-}\mu\text{m}$ results so they will not be presented here. The results for the HOPG and the stage-1 intercalated GIC are shown in Figs. 4 and 5, respectively. The shape of the reflectivity curve of the GIC (Fig. 5) is indeed consistent with the ideal reflectivity curve shown in Fig. 1(b). The reflectivity of the beam polarized in the plane of incidence has indeed a deep minimum. On the other hand, the reflectivity of the perpendicularly polarized radiation has a monotonic behavior. The reflectivity of the HOPG (Fig. 4) is substantially different. This is because the parallel dielectric constant of the graphite cannot be described by a plasma-type dielectric response.

Both reflection curves were fitted with calculated reflectivities using the components of the dielectric tensor and a minute air gap as parameters. It was found that even a very small gap between the graphite and the germanium, which can be hardly avoided, has a significant influence in the experiment on the reflectivity. The parameters for the HOPG are the following: $\epsilon_{\parallel r}^G = 3.0$; $\epsilon_{\parallel i}^G = -44.1$; $\epsilon_{\perp r}^G = 3.5$; $\epsilon_{\perp i}^G = -0.66$; the gap is $d = 0.09 \mu\text{m}$. The parameters for the GIC are the following: $\omega_p = 3.2 \text{ eV}$; $\gamma = 0.16 \text{ eV}$; $\epsilon_{\perp r}^G = 1.87$; $\epsilon_{\perp i}^G = -1.28$; The air gap $d = 0.135 \mu\text{m}$. From ω_p and γ one can calculate the parallel component of the dielectric tensor: $\epsilon_{\parallel r}^G = -110$ and $\epsilon_{\parallel i}^G = -74$.

We checked the fits for interdependences among the parameters and found one interdependence in the GIC sample and one in the HOPG. Therefore the value of one of the parameters in each sample was taken from previously published work. For ω_p we took an intermediate value between the results of Hanlon *et al.*¹² and Saint Jean *et al.*¹³ In the HOPG we took the value of $\epsilon_{\parallel i}^G$ from the work of Phillip.⁴ The fit results are shown in Figs. 4

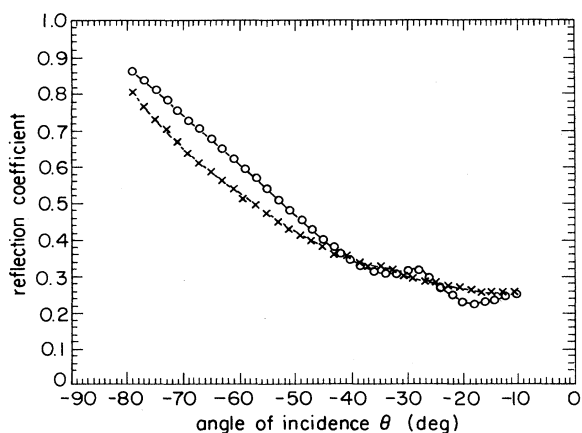


FIG. 4. The reflection coefficient as a function of the angle of incidence for HOPG. \circ , in-plane polarization; \times , out-of-plane polarization. The lines represent the theoretical fit (the parameters are discussed in the text).

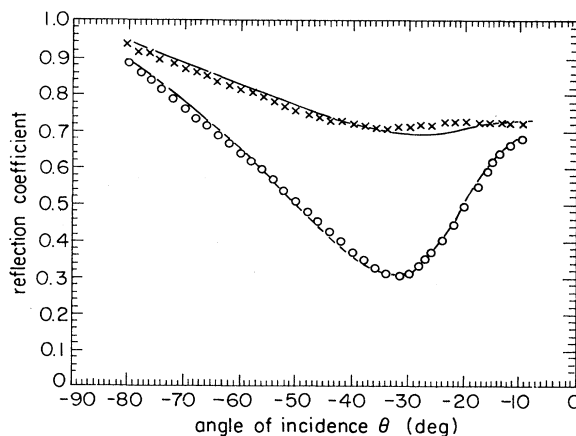


FIG. 5. The reflection coefficient as a function of the angle of incidence for stage-1 C/AsF₅ GIC. \circ , in-plane polarization; \times , out-of-plane polarization. The lines represent the theoretical fit (the parameters are discussed in the text).

and 5. All the features of all the curves are very well reproduced.

Using these parameters we can now evaluate numerically the sensitivities of the reflectivity to changes in the dielectric constant of the HOPG and the GIC. The results are shown in Fig. 6. The sensitivities are calculated for 5- and 15- μm ir light for the GIC and the HOPG samples. We show only the sensitivities for changes in the perpendicular components of the graphite dielectric constant because as expected the sensitivities to changes of the parallel component of the dielectric constant are negligible in comparison. Several features should be noted.

- The incidence angle at which the sensitivity is largest is almost independent of the wavelength.
- As expected, the sensitivity for light polarized in the plane of incidence is much larger than that for the out of plane polarization.
- In HOPG the sensitivity for changes in the imaginary part of the perpendicular dielectric constant is larger than for changes in the real part. The situation is reversed in the GIC sample. This feature will be important later on for the interpretation of the ir reflectivity spectra.

We also calculated the sensitivities of the air graphite reflection to changes in the graphite dielectric constant. At normal incidence they are at least 2 orders of magnitude smaller than the corresponding values of germanium graphite reflectivity. At 45° the ratio is seven.

In conclusion the sensitivity for observing the phonon contributions in ir reflectivity measurements from an interface between an ir transparent material and graphite at the proper angle is close to 2 orders of magnitude larger than that found in ordinary normal incidence reflectivity. Moreover, by properly choosing two appropriate measuring angles it is possible to determine the real and imaginary parts of the dielectric tensor contributed by the phonons.

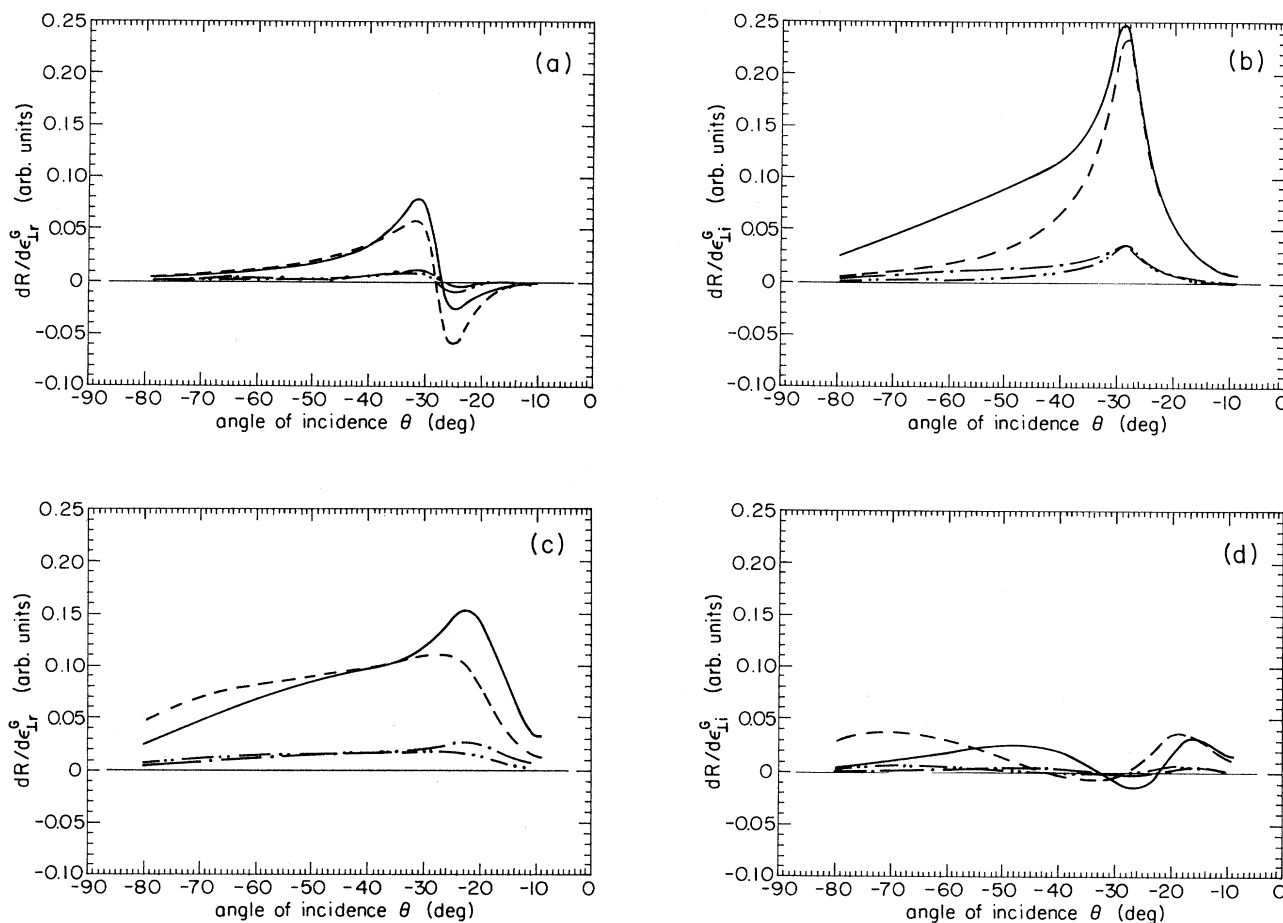


FIG. 6. The derivative of the reflectivity with respect to the real and imaginary parts of the perpendicular component of the dielectric tensors of graphite and of C/AsF₅ GIC as a function of the angle of incidence. The solid and the dashed lines are for the in plane polarization for 5 and 15 μm , respectively. The dashed-dotted and dashed-double-dotted lines are for the perpendicular polarization at 5 and 15 μm , respectively. (a) The derivative with respect to the real component of the dielectric tensor of graphite. (b) The derivative with respect to the imaginary component of the dielectric tensor of graphite. (c) The derivative with respect to the real component of the dielectric tensor of stage-1 C/AsF₅ GIC. (d) The derivative with respect to the imaginary component of the dielectric tensor of stage-1 C/AsF₅ GIC.

VI. SPECTRAL MEASUREMENTS OF THE IR REFLECTION IN THE RANGE OF THE VIBRATIONAL MODES

The ir-reflectivity spectra are measured *in situ* using the intercalation chamber shown in Fig. 2. The chamber is placed in the sample compartment of a fast-Fourier-transform ir spectrometer type Bruker IFS 113v. The ir beam emanating from the interferometer enters the germanium through the semicylindrical surface and is reflected from the sample at 45°. The reflected light goes out through the germanium and is detected by a silicon bolometer detector cooled to liquid-He temperature.

Each spectrum is obtained by taking the ratio between two reflectivity spectra. One with the sample pressed against the Ge crystal. The other is a reference spectrum measured with the graphite sample detached from the

Ge. The reflectivity at the Ge-air interface is equal to unity for angles larger than 14.5° because of total reflection. Thus this measurement is used in order to normalize the spectra of the graphite samples.

We performed a series of measurements starting with unintercalated HOPG followed by measurements on the AsF₅-intercalated graphite at various times of intercalation. In Fig. 7 we present the spectra between 825 and 900 cm^{-1} which include the ir-active mode of the pure graphite. Notice that soon after the intercalation starts, the reflectivity line shape of this mode changes from an almost absorption type profile to a dispersion-type profile. In addition as the intercalation progresses the intensity of the line decreases, a second line appears at 877 cm^{-1} , then the first line disappears altogether and finally the second line also disappears. The shape of the second line is the same as that of the first.

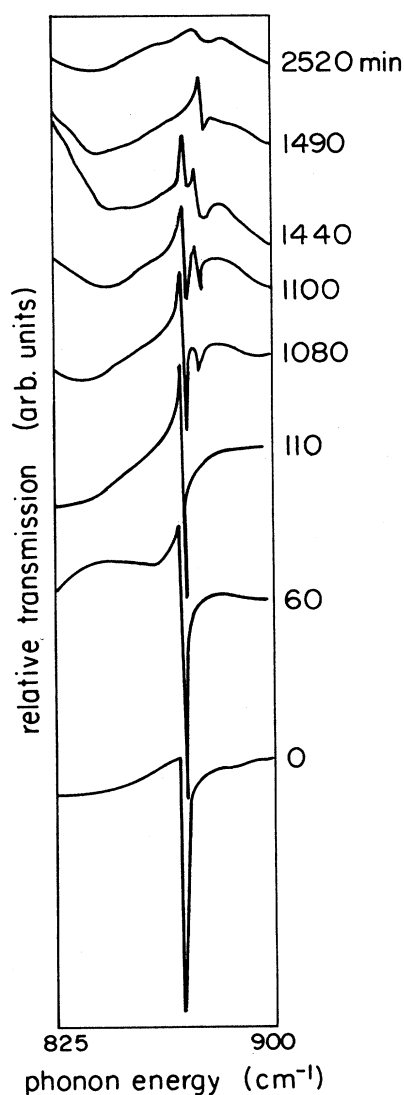


FIG. 7. Normalized reflectivity between 825 and 900 cm^{-1} for different intercalation times.

The ir spectrum between 600 and 900 cm^{-1} of stage-1 GIC is shown in Fig. 8. The structure observed is due to the intercalated graphite. The spectrum of the pure graphite in this range, is smooth except for the graphite line at 863 cm^{-1} . Reference spectra were taken during each intercalation step, when the graphite had to be removed temporarily from the germanium. These reference spectra did not change after the different steps, except for a small spectral feature near 638 cm^{-1} , probably from some specimens sticking on the germanium. We therefore disregard this feature in all spectra. Notice that the remaining spectrum consists essentially of a series of dispersion shaped lines. The interpretation of these lines will be discussed in Sec. V.

V. DISCUSSION

Each ir-active mode contributes a term ϵ^p to the dielectric tensor of the sample. The form of this term is

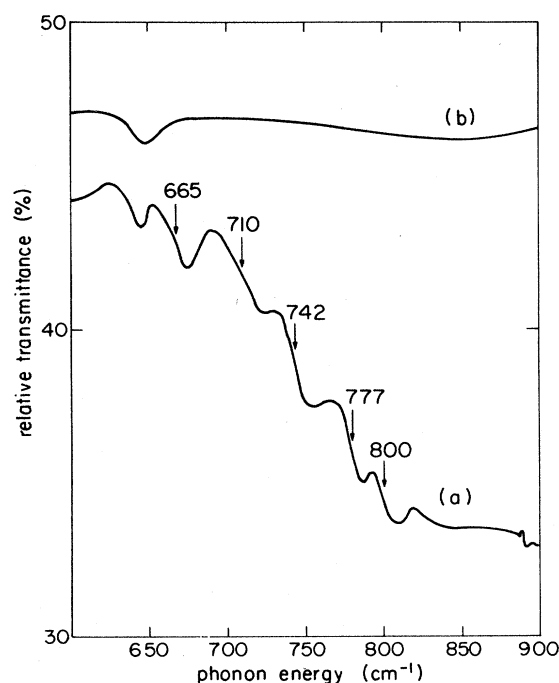


FIG. 8. (a) The normalized reflectance between 600 and 900 cm^{-1} . (b) The ratio between the reference spectrum at the start and the end of the intercalation process.

$$\epsilon^p = A / (\omega^2 - \omega_0^2 + i\omega\Gamma) . \quad (9)$$

The imaginary part of this contribution has the shape of a Lorentzian whereas the real part has the form of a dispersion curve. The sensitivity curves shown in Fig. 6 indicate that at an incidence angle of 45° the reflectivity of HOPG is much more sensitive to changes in the imaginary part than in the real part. Thus one would expect that for pure HOPG the phonon line shape will be close to a Lorentzian. On the other hand in the case of the GIC the reflectivity is sensitive almost exclusively to changes in the real part of the dielectric constant. Thus the line shape should be that of a dispersion curve. These features are indeed observed in both Figs. 7 and 8. As stated in Sec. III, the reflectivity is much more sensitive to changes in the perpendicular component of the dielectric tensor than in the parallel component. Thus, essentially only modes which are ir active in the C direction are expected to appear. In agreement with previous work,⁷ we attribute the appearance of a second graphite line to vibrations in the graphite bounding layer. Thus when only the second line is present the material is in stage 2.

The A_{2u} vibration is ir active only as long as there are at least two adjacent graphite layers involved. This mode of vibration becomes ir inactive when the graphite layer is sandwiched between two intercalant layers, assuming that the interaction between the graphite and the intercalant layers is very weak. This explains the disappearance of the A_{2u} line after a long time of intercalation, when the sample is presumably in stage 1.

TABLE I. The frequencies of ir-active modes of the different chemical species found in AsF₅ intercalated graphite.

Chemical species	Point group	Representation	In gas (cm ⁻¹)	In cond. matter (cm ⁻¹)	Present experiment (cm ⁻¹)
AsF ₃	C _{3v}	E	699 (Refs. 18 and 19)	644 (Ref. 19)	665
AsF ₃	C _{3v}	A ₁	738 (Refs. 18 and 19)	715 (Ref. 19)	710
AsF ₅	D _{3h}	A ₂ ''	784 (Ref. 20)		777
AsF ₅	D _{3h}	E'	811 (Ref. 20)		800
AsF ₆ ⁻	O _h	F _{1u}		699-710 (Ref. 21)	710
As ₂ F ₁₁ ⁻	D _{2h}			650-770 (Ref. 22)	742

According to our interpretation of the line shapes, the line positions should be measured at the points of largest slope. We observe five lines: P1-665, P2-710, P3-742, P4-777, and P5-800. In general, it is expected that upon intercalating graphite with AsF₅ a chemical reaction takes place producing AsF₃, AsF₅, and AsF₆⁻. Several authors,¹⁵⁻¹⁷ have suggested that in addition to these species there is also some As₂F₁₁⁻ present.

The frequencies of the different vibrational modes of these species in the gas and in condensed matter form are given in the range between 600 and 900 cm⁻¹ in Table I. Also shown in the table are the point symmetries of the species and their representations. It should be pointed out that the vibrational frequencies of ir-active modes are larger in the gas form than in the condensed matter form. The reason is that in the condensed form the dielectric surrounding the electrical dipole of the molecule reduces the electrostatic energy associated with it, thus reducing the effective force constant of the vibration. This in turn reduces the frequency of the vibration. Thus the frequencies we measure should be lower than the frequencies measured in the gas phase but may be slightly larger or smaller than the frequencies measured in the condensed matter form (these values depend on the specific system involved). Using these considerations and the values listed in the table we have suggested a *tentative* interpretation of the observed lines. This is shown in the last column of Table I. These results strongly confirm what has been known from chemical considerations namely that AsF₅ intercalated graphite contains also AsF₃, AsF₆⁻, and possibly As₂F₁₁⁻.

VI. SUMMARY AND CONCLUSIONS

The ir reflectance at an interface between an infrared transparent material and a graphite sample has been analyzed. It is shown that, under certain conditions part of the ir radiation penetrates into the graphite sample and propagates in it even if the optical dielectric constant of

the graphite parallel to its surface is negative. The conditions are as follows.

- The light is polarized in the plane of incidence.
- The optical dielectric constant of the IRTM is larger than the perpendicular component of the graphite dielectric tensor.
- The angle of incidence is larger than a critical angle.

We also calculate the sensitivity of such a reflectance measurement to phonon contributions and we show that it has a peak close to the critical angle. The sensitivity at the peak is larger than the sensitivity of ordinary reflectivity at an air graphite interface at normal incidence by more than 2 orders of magnitude. Measurements of the reflectivity as a function of the angle of incidence support these conclusions and provide the values of three out of the four dielectric components of the graphite.

To demonstrate the power of this technique we measured the ir reflectivity spectra of graphite intercalated with AsF₅. The measurements were done *in situ* and show the evolution of the A_{2u} graphite line with intercalation time. In addition five intercalant lines are observed for the first time by ir reflectivity.

This method opens up the way to study systematically intercalant vibrations in any acceptor type GIC's. Moreover the fact that it can be done *in situ* provides the possibility to study various structural phase transitions through their effects on the dynamical properties of the graphite layers and the intercalants.

ACKNOWLEDGMENTS

One of us is deeply indebted for broad discussions with Professors Mili and Professor Gene Dresselhaus. We thank A. W. Moore for supplying us with the HOPG samples. It is a pleasure to acknowledge the support of the U.S.-Israel Binational Science Foundation (Jerusalem, Israel) under Grant No. 86-00131/1 and the Deutsche Forschungsgemeinschaft (Bonn, West Germany).

*Also at The Racach Institute of Physics, The Hebrew University of Jerusalem, Givat Ram, 91 904 Jerusalem, Israel.

¹I. Ohana and Y. Yacoby, Phys. Rev. Lett. **57**, 2572 (1986).

²M. S. Dresselhaus and G. Dresselhaus, in *Light Scattering in Solids*, edited by M. Cardona and G. Guntherödt (Springer,

New York, 1982), Pt. 3, p. 3.

³L. J. Brillson, E. Burstein, A. A. Maradudin, and T. Stark, in *Proceedings of the International Conference on Semimetals and Narrow Gap Semiconductors*, edited by P. L. Carter and R. T. Bate (Pergamon, New York, 1971), p. 187.

- ⁴R. J. Nemanich, G. Lucovsky, and S. A. Solin, *Solid State Commun.* **23**, 117 (1977); *Mater. Sci. Eng.* **31**, 157 (1977).
- ⁵C. Underhill, S. Y. Leung, D. Dresselhaus, and M. S. Dresselhaus, *Phys. Rev. B* **31**, 2451 (1985).
- ⁶S. Y. Leung, G. Dresselhaus, and M. S. Dresselhaus, *Solid State Commun.* **38**, 175 (1981).
- ⁷M. P. Conrad and H. L. Strauss, *Phys. Rev. B* **31**, 6669 (1985).
- ⁸R. Al-jishi and G. Dresselhaus, *Phys. Rev. B* **26**, 4523 (1982).
- ⁹H. Zabel, *Physica B & C* **136B**, 1 (1986).
- ¹⁰P. C. Eklund, N. Kambe, G. Dresselhaus, and M. S. Dresselhaus, *Phys. Rev. B* **18**, 7069 (1978).
- ¹¹A. Erbil, G. Dresselhaus, and M. S. Dresselhaus, *Phys. Rev. B* **25**, 5451 (1982).
- ¹²L. R. Hanlon, E. R. Falardeau, and J. E. Fischer, *Solid State Commun.* **24**, 377 (1977).
- ¹³M. Saint Jean, Nguyen Hy Hau, C. Rigaux, and G. Furdin, *Solid State Commun.* **46**, 55 (1983).
- ¹⁴H. Philipp, *Phys. Rev. B* **16**, 2896 (1977).
- ¹⁵L. W. Ebert, D. R. Mills, J. C. Scanlon, and H. Selig, *Mater. Res. Bull.* **16**, 831 (1981).
- ¹⁶S. Brownstein, *Can. J. Chem.* **47**, 605 (1969).
- ¹⁷M. Lelaurain, J. F. Mareche, E. McRae, G. Furdin, and A. Herold, *J. Mater. Res.* **3**, 87 (1988).
- ¹⁸L. C. Hoskins and R. C. Lord, *J. Chem. Phys.* **43**, 155 (1965).
- ¹⁹J. Weidlein, thesis, Universität Stuttgart, 1964 (unpublished).
- ²⁰L. C. Hoskins and R. C. Lord, *J. Chem. Phys.* **46**, 2402 (1967).
- ²¹G. M. Begun and A. C. Rutenberg, *Inorg. Chem.* **6**, 2212 (1967).
- ²²P. A. W. Dean, R. J. Gillespie, and R. Hulme, *J. Chem. Soc. Chem. Commun. No. 17*, 990 (1969).